

UIIU-ENG 86-3606

Report No. 129

CHARACTERIZATION OF Fe-Cr-Ni ALLOYS PRODUCED BY
LASER SURFACE ALLOYING USING MIXED POWDER FEED

by

T. Chande, A. Ghose and J. Mazumder
Department of Mechanical and Industrial Engineering

A Report of the

MATERIALS ENGINEERING - MECHANICAL BEHAVIOR

College of Engineering, University of Illinois at Urbana-Champaign

July 1986

CHARACTERIZATION OF Fe-Cr-Ni ALLOYS PRODUCED BY
LASER SURFACE ALLOYING USING MIXED POWDER FEED

T. Chande*, A. Ghose**, and J. Mazumder***
Department of Mechanical and Industrial Engineering
1206 West Green Street
University of Illinois at Urbana-Champaign
Urbana, IL 61801

ABSTRACT

A new screw-fed, gravity-flow, carrier-gas aided powder delivery system was used to make laser surface alloys using Cr and Ni powders on AISI 1016 steel. A 10 kW CW CO₂ laser was used for alloying, at incident power densities up to 2×10^7 W/m² and traverse speeds up to 0.03 m/s. Ten overlapped passes were used to make alloyed zones 0.05 m long by 0.015 m wide. Alloys with up to 80 weight percent Cr and 58 percent Cr + 26 percent Ni were obtained. Surface roughness and corrosion resistance measurements were made. The microstructure was characterized by transmission and scanning electron microscopy. Smoother surfaces were obtained by increasing traverse speed and beam diameter. Corrosion samples passivated spontaneously in a 3.5 percent NaCl solution in distilled water, but were susceptible to pitting corrosion when uneven surfaces were subjected to corrosion testing. Microstructures were highly refined with a high dislocation density. These results are related to process mechanisms. The reported method of powder delivery is versatile, flexible and reproducible, and can be used to make useful alloys.

* Formerly Graduate Research Assistant at UIUC; presently member of Technical

Staff, General Electric Corporate Research and Development Center, Schenectady, New York.

** Formerly Visiting Assistant Professor at UIUC; presently at National Metallurgical Laboratory, India.

*** Associate Professor, Materials and Design Division.

Introduction

Laser Surface Alloying (LSA) is a process for producing uniformly alloyed surface layers. However, LSA has not been systematically examined, nor have the resultant materials been fully characterized [1,2]. As a part of our continuing study of LSA, a new powder delivery system has been used to produce alloys of Fe + Cr and Fe + Cr + Ni. The production of these alloys and the observed microstructures are described and the measured surface properties are presented.

The use of powders in laser surface modification has been reported by several authors. Gnanamuthu [3] applied Ni and Cr powders to steel substrates as a slurry or by spraying. To create mixing and minimize porosity, this method required high powers (12.5 kW) or beam oscillation at lower powers (< 6 kW). A specially designed nozzle was used by Ayers [4] to inject Si powder into the molten-pool while alloying 5052 Al. Processing was done at ambient pressure in an environmental chamber using a helium gas shield and alloyed traces had to be remelted four times for homogenization. A mechanically vibrated gravity-flow system that worked for a specific range of powder sizes was used by Breinan, et al. [5], to build-up layers by laser melting. They also tried wire feed but laser coupling was better with powder feed. Laser cladding was done using a modified spray-gun by Powell and Steen [6]. Powder feed rates were varied by changing the carrier-gas flow rate.

Some surface property measurements are available. Moore, et al. [7], investigated surface roughness in several laser melted metals at high power densities (10^{11} W/cm²) and short interaction times (0.1-1.2 ms). They suggest that under these conditions, surface roughness can be reduced by decreasing laser power and speed. Esquivel, et al. [8], report surface roughness measurements at low powers and high speeds up to 111 cm/s. They found surface

rippling at all speeds and predict that it cannot be eliminated even at very high speeds due perhaps to non-steady-state surface tension driven convection. The corrosion resistance of laser surface alloyed Fe + Cr alloys has been measured by Moore and McCafferty [9] in Na_2SO_4 while Lumsden, et al. [10], used 1N H_2SO_4 for testing Fe + Cr + Ni alloys. Both found the corrosion resistance of laser alloys to be far superior to that of the substrate.

The objectives of the present work were to develop a flexible system for powder delivery and use it to prepare ferrous surface alloys using Ni and Cr powders. Surface roughness and corrosion resistance were to be measured and the microstructure characterized. Reproducibility was to be assessed and the observed results related to processing conditions and mechanisms.

Experimental Procedure and Methods

A 10 kW CW CO₂ laser was used for the runs. During laser processing, a closed loop monitor was used for continuous sampling of output power using a fast infra-red detector and adjustment of electrical input to the laser to maintain a constant ± 3 percent output power. A He-Ne laser was used to align the powder delivery system and position the sample for overlapping traces. The sample was placed on a table capable of x-y-z movement. Table speed was measured by timing its traverse over a preset distance. Beam diameter was set to obtain melt-widths of about 3 mm. An overlap of approximately 50 percent was used for all the samples. A gas shield (Fig. 1) was used to minimize oxidation of the sample and combustion of powder particles under the laser beam. A flow of helium gas at 1.13 to 1.7 m³/hr (40 to 60 ft³/hr) was piped into the shield. Argon gas-assist for powder feed was set at 0.085 to 0.14 m³/hr (3 to 5 ft³/hr). Helium was fed into the shield for 45 seconds prior to initiation of a run and Ar for 15 seconds.

Commercially available Cr powders, 2 μ m in diameter, and Ni powders, 5 μ m in diameter, were used. They were baked to remove moisture. A mixture of 50 percent by weight of the two powders was used to produce the ternary Fe-Cr-Ni alloys. Powders were dropped into a delivery chute by a screw-feeder. The delivery system used 10 mm bore copper tubing with 10 mm bore flexible polymer tubing used to make connections requiring small bends. Powders were deposited at the point of laser-material interaction. The end of the copper delivery tube was sawed off at about 45 degrees to facilitate powder discharge and was positioned about 8 mm ahead and 15 mm above the point of laser material interaction. If the tube was too close to the point of laser-material interaction, it could be damaged by direct irradiation or the powder flow could be blocked by fused powders.

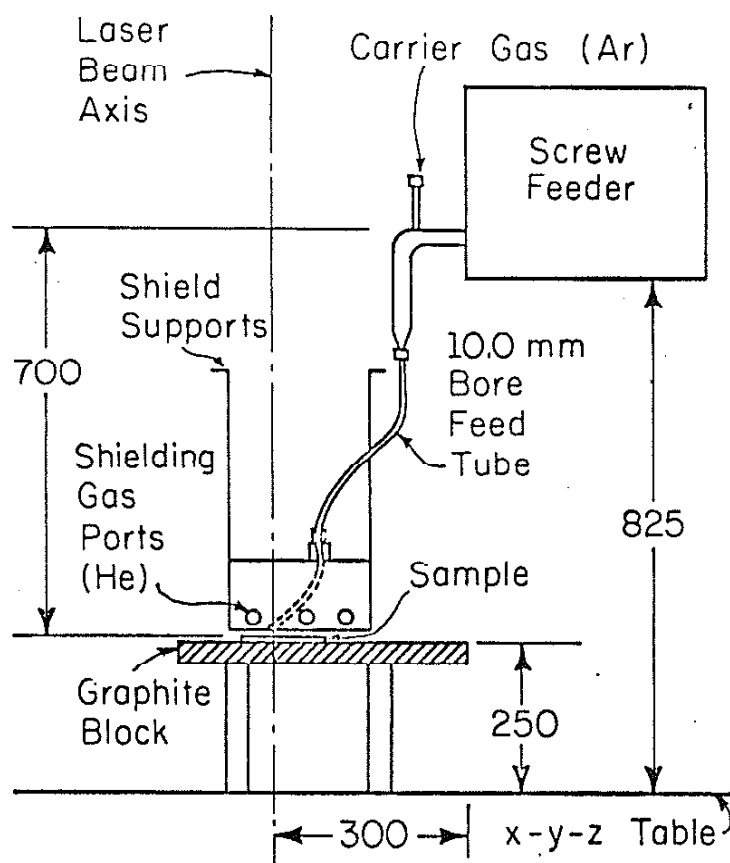


Figure 1 Schematic diagram of screw-fed, gravity-flow, carrier gas-aided powder delivery system. All dimensions are in mm.

Bars of AISI 1016 steel were used for the runs. These were 150 mm long, 50 mm wide, and 6 mm thick. The bars were bolted onto another bar of 1016 steel, 8 mm thick, to reduce warping during laser processing. Up to 10 overlapped alloying traces were made to coat an area approximately 15 mm wide and 50 mm long.

Samples were cut 10 mm from the ends for metallurgical examination of the transverse section of laser alloys. Corrosion samples were made from the portion between 10 and 25 mm from the edge. TEM foils were made from the 10 mm of alloyed zone adjacent to the corrosion samples.

Corrosion samples, 15 mm in diameter and 2 to 3 mm thick, were made by grinding a 15 mm square section. The LAZ surface was lightly ground to 600 grit paper to produce an approximately flat surface. It was desired to test alloys in the as-prepared condition; thus, the samples had an uneven surface, not completely without surface imperfections. A few samples had short, shallow, uneven "grooves" on the surface. An O ring, 9.25 mm internal diameter and 1.78 mm wall thickness was glued to the sample surface using quick-drying adhesive to prevent the corrosive solution from seeping out from under the O ring at surface irregularities and attacking the base material at the back of the sample. This portion, except for a small area left bare for electrical contact with testing system, was painted using a commercial nail-polish enamel to prevent inadvertent attack by the solution.

Corrosion tests were made using a Princeton Applied Research corrosion system, consisting of a Model 175 Universal Programmer, a Model 173 Potentiostat/Galvanostat, with a Model 376 Logarithmic Current Conversion module. A standard three-electrode Greene Cell was used. Approximately 800 ml of the 3.5 percent sodium chloride solution stirred at a constant velocity in distilled water was used in these tests. The electrolyte was not deaerated. Po-

tentiodynamic anodic scans were made at 0.36 v/hr, the potential being measured versus a saturated calomel electrode (SCE). Scans began at the stabilized corrosion potential after a 30 minute immersion in solution and were terminated after scanning over a 2 Volt range.

Surface roughness measurements were made using a Rank Taylor Hobson Taly-surf 10 surface texture measuring instrument. A low magnification pick-up with a 12.5 μm tip radius diamond stylus was used. Meter cut-off was 0.8 mm with a vertical magnification of 200X, a horizontal magnification of 100X, and a horizontal traverse speed of 0.5 mm/s. The measured profile was digitized using an analog-digital converter at a sampling rate of 100 points/s. A typical traverse had up to 1,000 data points. The data were analyzed to calculate the roughness average, R_a . The measurements were made on previously prepared laser surface alloys of Fe-Cr-Ni made according to a 2^3 factorial experimental design plan [1]. The computed R_a values were statistically analyzed to quantify the effect of varying process variables upon surface roughness.

During surface alloying, based on previous results [1], operating conditions were chosen to obtain a depth greater than 0.5 mm. Screw feed, which could be dialed in between 000 to 999 was set at 800 to 999, with the higher feed rates being used with conditions that were expected to produce greater depths. The variation of power density and speed were usually in the form of a 2^2 factorial design. Alloys were sectioned after processing for metallurgical examination.

Electron-probe microanalysis was used to measure compositions of laser alloyed zones. Alloying was generally uniform and diffusion of alloyed species across the solid-liquid interface was negligible. X-ray photon count maps were also used to check uniformity of mixing. Sections of LAZ about

100 μm below the surface were prepared for examination in a Phillips 400 TEM. A 5 percent solution of perchloric acid in methanol was used in a twin-jet polisher to prepare the thin foils.

Results of Experiments

Compositions obtained by laser surface alloying are summarized in Table 1. Roughness average values determined from digitized traces (as shown in Fig. 2) were statistically analyzed and the main and interaction effects deduced and plotted under a reference t-distribution (Fig. 3) to determine their significance. The traces had an average R_a value of 29.3 μm . The roughness average R_a decreased with an increase in traverse speed and beam diameter. An increase in speed from 25 to 50 mm/s decreased average roughness by 14.8 μm ; increasing the beam diameter from 0.8 to 1.28 mm decreased R_a values by 11.8 μm on the average.

All laser alloyed samples passivated spontaneously (Fig. 4) in 3.5 percent salt solution and had a current density in the passive state equal to or greater than that recorded for AISI 304 stainless steel. The pitting potentials recorded for laser alloyed samples were generally more active than that recorded for 304 stainless steel.

Uniformity of alloying was checked using electron probe microanalysis. Figure 5 shows the chromium variation across a typical laser surface alloyed sample as determined by electron probe microanalysis.

Examination of thin foils in a transmission electron microscope (TEM) showed several interesting microstructures. Featureless amorphous regions were seen in a LAZ made at low power density ($0.8 \times 10^6 \text{ W/cm}^2$) and a traverse speed of 50 mm/s (Figs. 6 and 7). An electron energy loss spectrograph of this foil showed very little oxygen. A scanning Auger analysis indicated presence of phosphorus, estimated to be between 8 to 18 weight percent (Fig. 8). Since the Fe-P system has a deep eutectic at 10 weight percent P and as the glass-forming tendency increases with addition of alloying elements [11], these amorphous regions were considered to be Fe-P alloys. Clearly,

Table 1 Average Composition of Fe + Cr + Ni Alloys by EPMA

<u>Laser Power</u> (kW)	<u>Speed</u> (mm/s)	<u>Feed Rate</u> g/s	<u>Cr</u> <u>wt-pct</u>	<u>Ni</u> <u>wt-pct</u>
6	16.5	0.25	22.1	17.2
5	16.5	0.25	35.1	25.5
5	16.5	0.25	38.3	23.7
6	20.7	0.18	13.1	10.1
6	20.7	0.19	16.3	12.3
6	24.9	0.2	28.4	19.5
6	29.5	0.2	34.8	23.3
5	24.8	0.2	37.6	21.8

The first three alloys were made with a delivery tube 10 in. internal diameter; the rest with a tube 7.5 mm internal diameter. Beam diameter was about 2 mm for all runs.

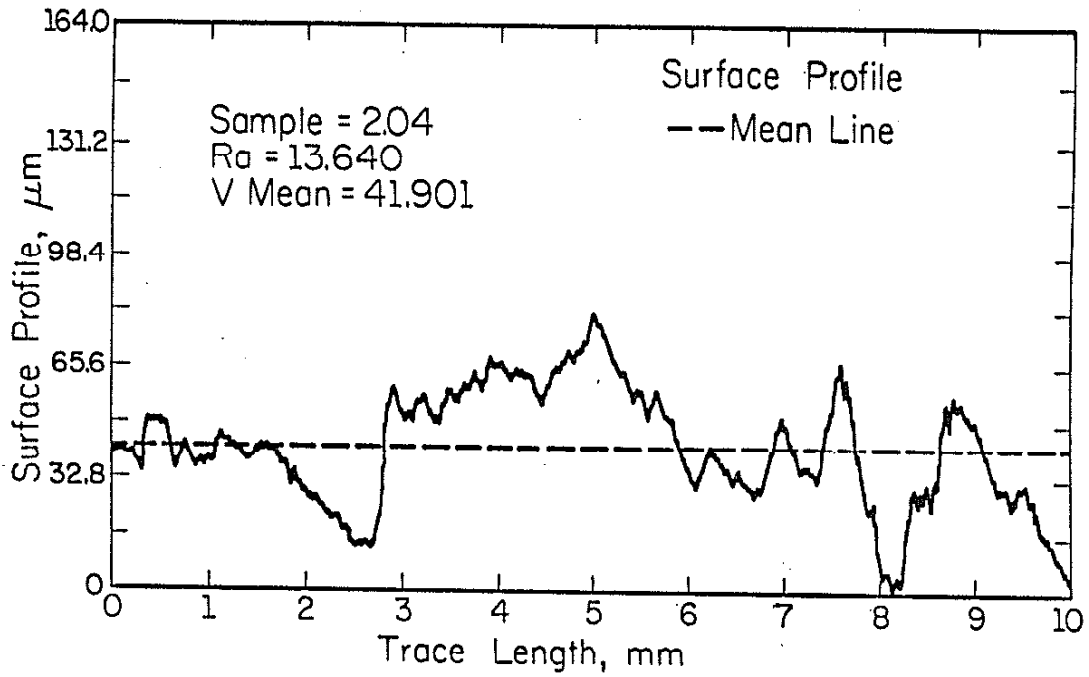


Figure 2 Typical surface texture measurement trace on Fe + Ni alloy.

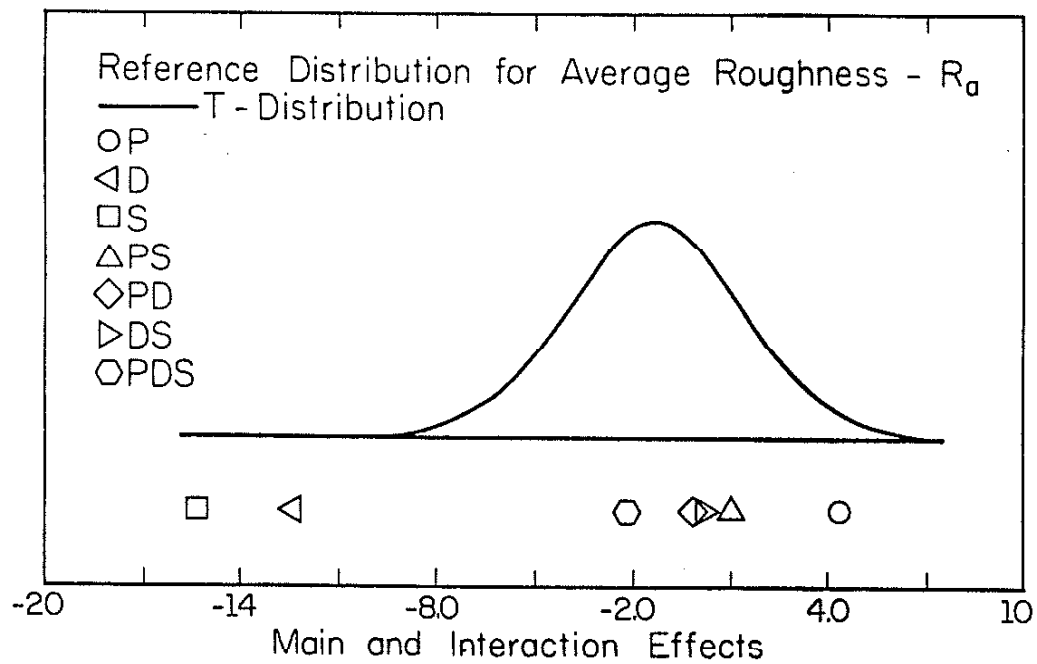


Figure 3 Reference t-distribution for main and interaction effects for roughness average values obtained from Fe+Ni alloys. Effects that lie to the edges of the distribution are statistically significant. (P = laser power, W; D = beam diameter, m; S = traverse speed, m/s; PD = 2-factor interaction; PDS = 3-factor interaction).

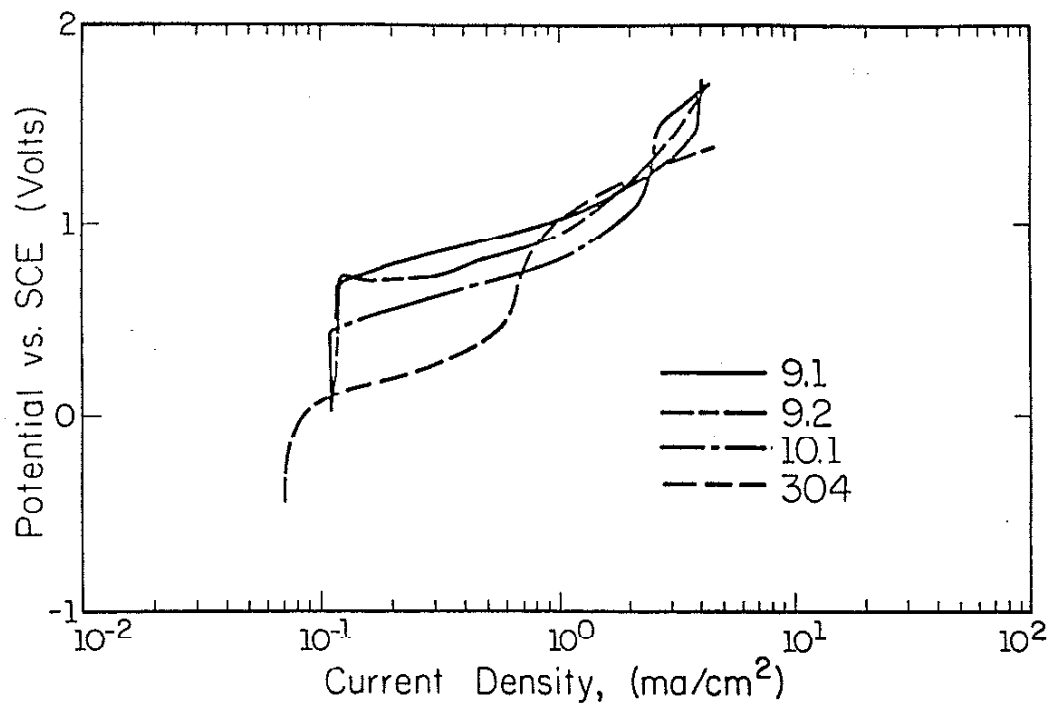


Figure 4 Anodic potentiodynamic scans for laser processed samples and bulk 304 stainless steel in 3.5 percent salt solution. (Average compositions in weight percent are: 9.1= 22 Cr, 17 Ni; 9.2 = 35 Cr, 26 Ni; 10.1 = 13 Cr, 10 Ni).

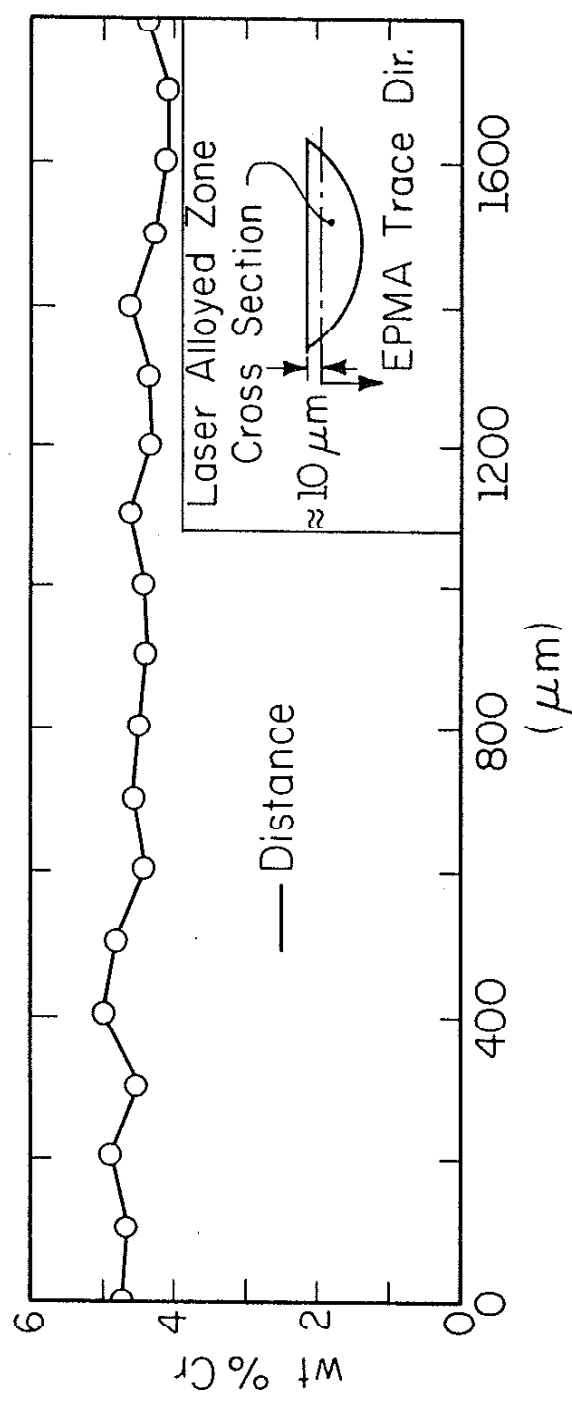


Figure 5 Distance across the transverse section of the LAZ near surface. EPMA trace is made closest to the surface, within 10 μm.

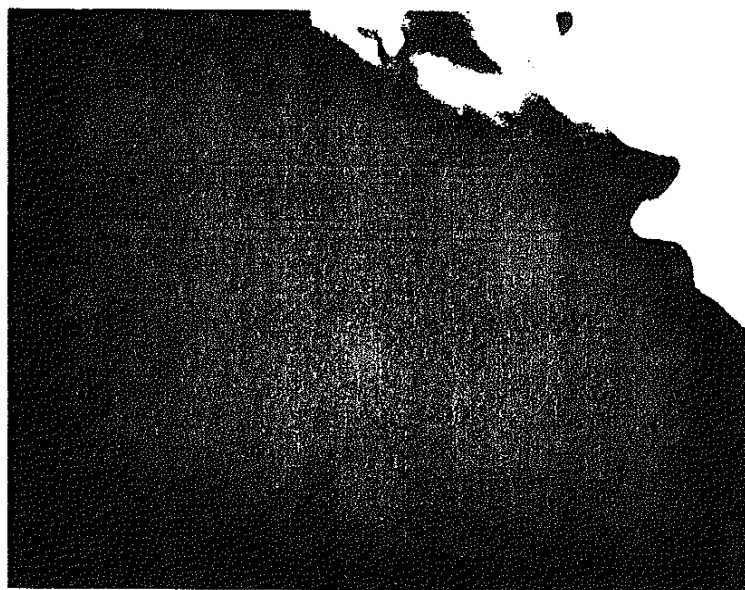


Figure 6 Featureless region from near top surface of an LAZ processed at laser power of 4 kW, 1.28 mm beam diameter and 50 mm/s traverse speed.

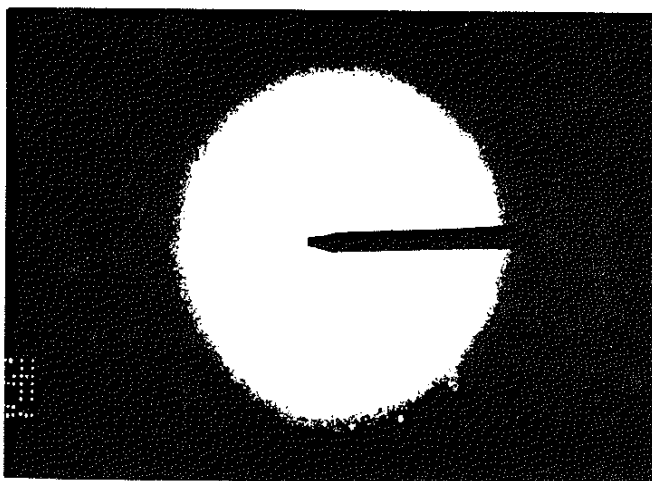


Figure 7 Selected area electron diffraction pattern from area in Fig. 8 showing diffuse rings.

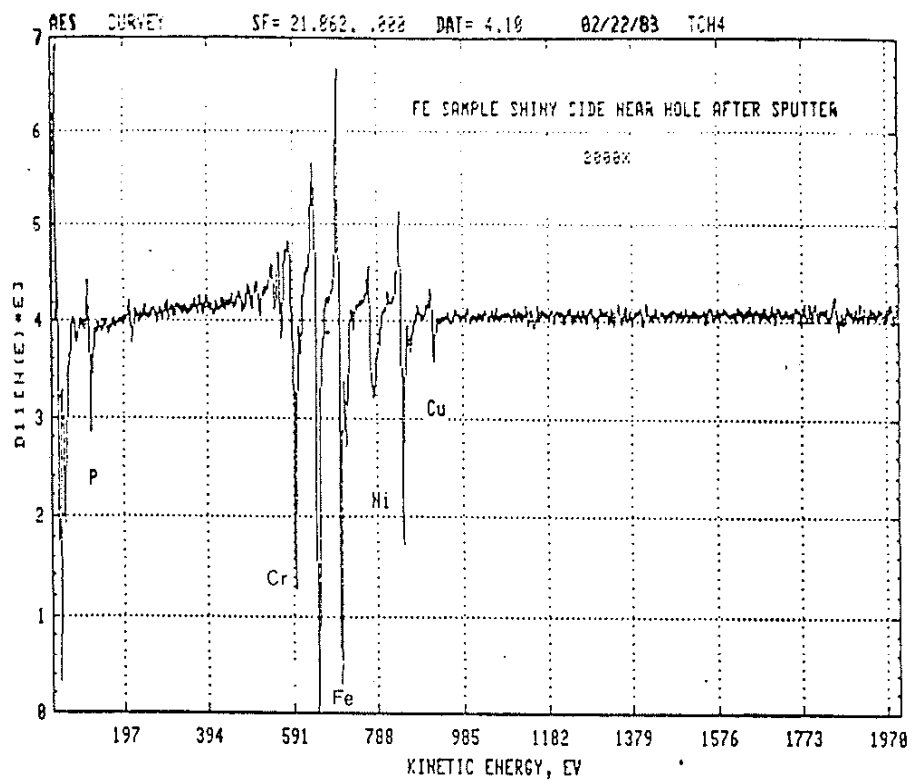


Figure 8 Auger scan from foil in Fig. 6 showing presence of P.

these regions were formed by a combination of suitable composition and high cooling rates.

Cr-rich, blocky precipitates were observed at grain boundaries (Fig. 9). A highly dislocated lath microstructure with a BCC structure was commonly seen (Fig. 10). Diffraction patterns for these foils did not show any orientation relationships between the laths. These observations are generally characteristic of low-carbon steel quenched structures [12]. The presence of preferred orientation was seen in another foil while several foils also showed the presence of micro-crystalline areas.

An optical examination of the LAZ's showed that the highly alloyed Fe-Cr alloys were difficult to etch and had a grain size about 11 times greater than that seen in the Fe-Cr-Ni alloys. A high degree of refinement was observed in some of the Fe + Ni alloys showing structures on the scale of 5 nm (Fig. 11), most probably this is due to micro-twinning.



Figure 9 Cr-rich grain boundary precipitates at a depth below 375 μm from the surface in sample made at 6 kW laser power, 3 mm beam diameter and 12.7 mm/s traverse speed with Cr powder feed.



Figure 10 Dislocated lath structure from a laser alloy with 12.5 percent Cr and 1.5 percent Ni that showed BCC single-crystal diffraction pattern and no orientation relationships between laths.



Figure 11 Very fine, plate structures seen in LAZ of bead of Fe + 0.5 Ni in laser alloy made at 6 kW laser power, 0.8 mm beam diameter and 25 mm/s traverse speed.

Discussion of Results

The wide range of observed compositions indicates the versatility of using a powder feed for laser surface alloying. Alloying is fairly uniform and the phase diagram does not pose limits to the creation of alloys. In agreement with our previous results [1], as melt volume decreases for a given rate of supply of alloying elements or as the rate of supplying alloying additions increases for a given melt volume, the average solute content increases.

The present powder dispensing system is simple, flexible in terms of powder sizes that can be fed, achieves a good range of powder feed rates and provides effective shielding at ambient pressures. The effectiveness of the shielding arrangement can be further improved simply by increasing gas flow rates. Virtually any mix of powders can be fed to produce a desired alloy composition. Also, pools as deep as 1.5 mm can easily be highly alloyed in a single pass using power densities on the order of 2×10^7 W/m². Such depths permit design of post-alloying machining procedures if required.

Surface roughness depends on the vigor of fluid flow in the melt pool. As traverse speed increases, or beam diameter increases, temperature gradients in the pool become less steep. This reduces surface-tension gradients across the width of the pool and reduces velocity of cross-flow. This results in an overall reduction in the vigor of fluid flow in the melt pool [13,14] leading to smoother surfaces upon solidification. The recommendations of Moore, et al. [7], are contradicted by these findings. They recommend a run at lower speed and powers to reduce surface roughness. While their recommendation about laser power lends some support to our data, that for speed does not.

Corrosion results imply that the LAZ's were sufficiently alloyed (>12% Cr) and did not have cracks that would expose the unalloyed base material to the corrosive solution. Examination of corrosion tested specimens

showed that pitting and exfoliation were probably the failure mechanisms. The more active pitting potentials shown by the laser alloyed specimens suggest that their passive film breakdown mechanism is different from that occurring on the 304 stainless steel and the uneven surface may well be conducive to local pitting. Usefulness of these alloys could be increased by alloying deep layers and grinding the surface of the LAZ to produce a flat, flaw-free surface.

The observed microstructures are a function of both composition and cooling rate. With a suitable composition, amorphous materials can be made at fairly modest cooling rates (up to a few million degrees a second). Cooling rates increase as solidification proceeds towards the surface [15] and, as seen here, amorphous material is expected at the top rather than the bottom of the pool. With the large amounts of Cr in the solution and the 0.16 percent carbon in the base material, precipitation of Cr-rich precipitates is possible at grain boundaries. The sample showing lath structure but the lack of orientation relationship between laths had about 12 percent by weight of Cr (Fig. 10). It must have passed through the $\gamma + \alpha$ region and the lack of orientation relationship probably means the laths were separated by low angle boundaries [12]. The commonly seen large dislocation density in the foils is to be expected in rapidly solidified steels. Large grains high in Cr, Fe-Cr alloys could occur if they formed at high temperatures during solidification. There are no solid-state transformations that could occur at high cooling rates to refine the microstructure, and the large grains would be retained at room temperature. This would also explain the lack of segregation and the resultant difficulty in developing the microstructure during etching.

It is worth noting that alloys with 58 percent Cr, 26 percent Ni were produced. Mixing due to convection plays a major role in producing such

highly alloyed structure [16]. Not only would such alloys have good oxidation resistance at elevated temperatures but their susceptibility to Cr depletion at grain-boundaries would be lower as there is enough Cr within the bulk of the grain to diffuse to the grain-boundary and compensate for Cr depletion.

Conclusions

The following conclusions were drawn from the results and discussion presented above:

1. Powder feed is a versatile and flexible method of producing laser surface alloys.
2. The new powder delivery system described here can be used reproducibly for laser surface alloying.
3. Surface roughness of laser alloyed zones can be decreased by increasing the traverse speed or beam diameter.
4. Laser surface alloys, with substantial amounts of Cr and Ni passivate spontaneously in a 3.5 percent sodium chloride solution, but may be susceptible to pitting when used in the as-prepared condition.
5. Depending on the composition and cooling rates, a variety of refined microstructures including amorphous structures are obtained in laser surface alloys.

Acknowledgments

This work was supported by the American Iron and Steel Institute under Grant AISI 62-443 and the University of Illinois Materials Processing Consortium. A portion of the microstructural analysis reported here was conducted in the Center for Microanalysis of Materials, Materials Research Laboratory, University of Illinois at Urbana-Champaign. Corrosion tests were performed at the U.S. Army Construction Engineering Research Laboratory, Champaign, Illinois. Cooperation and valuable help from Ms. E. Segan of CERL is acknowledged. The cooperation and advice of Mr. T. S. Babin in conducting surface roughness measurements is also gratefully acknowledged.

References

1. T. Chande and J. Mazumder: Metall. Trans. B, 14B(2), 1983, pp. 181-190.
2. C. W. Draper: Laser in Metallurgy, K. Mukherjee and J. Mazumder, eds.; 1981 AIME, Warrendale, PA, pp. 67-92.
3. D. S. Gnanamuthu: Optical Engineering, 19(5), 1980, pp. 783-799.
4. J. D. Ayers: Thin Solid Films, 84, 1981, pp. 323-331.
5. E. M. Breinan, D. B. Snow, C. O. Brown and B. H. Kear: Rapid Solidification Processing Principles and Technologies II, R. Mehrabian, B. H. Kear and M. Cohen, eds.; pp. 440-452, Claitor's Publishing Division, Baton-Rouge, LA, 1980.
6. J. Powell and W. M. Steen: Lasers in Metallurgy, K. Mukherjee and J. Mazumder, eds.; pp. 93-104, AIME, Warrendale, PA, 1981.
7. P. Moore, C. Kim and L. S. Weinman: Applications of Lasers in Materials Processing, E. A. Metzbower, ed.; pp. 221-224, ASM, Metals Park, OH, 1979.
8. O. Esquivel, J. Mazumder, M. Bass, and S. Copley: Int. Conf. on Rapid Solidification, Processing Principles and Technologies, II, R. Mehrabian, B. H. Kear, and M. Cohen (eds.), Claitor Publishing, Baton Rouge, LA, 1980, pp. 180-188.
9. P. G. Moore and E. McCafferty: J. Electrochem. Soc., 128, 1981, pp. 1391-1393.
10. J. B. Lumsden, D. S. Gnanamuthu and R. J. Moores: Corrosion of Metals Processed by Directed Energy Beams, C. R. Clayton and C. M. Preece, eds; pp. 129-134, AIME, Warrendale, PA, 1982.
11. H. S. Chen, and K. A. Jackson: Metallic Glasses, J. J. Gilwan, and H. J. Leamy, eds. pp. 74-76, ASM, Metals Park, OH, 1978.
12. A. R. Marder, and G. Krauss: Trans. ASM, Vol. 60, 1967, pp. 657-660.
13. T. Chande and J. Mazumder: Appl. Phys. Letts., 41(1), 1982, pp. 42-43.
14. C. Chan, J. Mazumder, and M. M. Chen, Met. Trans. A, Vol. 15A(12), p. 2175, 1984.
15. J. A. Sekhar, S. Kou, and R. Mehrabian: Metall. Trans. A, 14A(6), 1983, pp. 1169-1177.
16. T. Chande and J. Mazumder, J. Appl. Physics, Vol. 57(6), pp. 2226-2232, 1985.

LIST OF FIGURES

Figure 1 Schematic diagram of screw-fed, gravity-flow, carrier gas-aided powder delivery system. All dimensions are in mm.

Figure 2 Typical surface texture measurement trace on Fe + Ni alloy.

Figure 3 Reference t-distribution for main and interaction effects for roughness average values obtained from Fe + Ni alloys. Effects that lie to the edges of the distribution are statistically significant. (P = laser power, W; D = beam diameter, m; S = traverse speed, m/s; PD = 2-factor interaction; PDS = 3-factor interaction).

Figure 4 Anodic potentiodynamic scans for laser processed samples and bulk 304 stainless steel in 3.5 percent salt solution. (Average compositions in weight percent are: 9.1 = 22 Cr, 17 Ni; 9.2 = 35 Cr, 26 Ni; 10.1 = 13 Cr, 10 Ni).

Figure 5 Distance across the transverse section of the LAZ near surface. EPMA trace is made closest to the surface, within 10 μm .

Figure 6 Featureless region from near top surface of an LAZ processed at laser power of 4 kW, 1.28 mm beam diameter and 50 mm/s traverse speed.

Figure 7 Selected area electron diffraction pattern from area in Fig. 8 showing diffuse rings.

Figure 8 Auger scan from foil in Fig. 6 showing presence of P.

Figure 9 Cr-rich grain boundary precipitates at a depth below 375 μm from the surface in sample made at 6 kW laser power, 3 mm beam diameter and 12.7 mm/s traverse speed with Cr powder feed.

Figure 10 Dislocated lath structure from a laser alloy with 12.5 percent Cr and 1.5 percent Ni that showed BCC single-crystal diffraction pattern and no orientation relationships between laths.

Figure 11 Very fine, plate structures seen in LAZ of bead of Fe + 0.5 Ni in laser alloy made at 6 kW laser power, 0.8 mm beam diameter and 25 mm/s traverse speed.